The ISME Journal (2019) 13:2107–2119
https://doi.org/10.1038/s41396-019-0425-9

ARTICLE

CO_2 conversion to methane and biomass in obligate methylotrophic methanogens in marine sediments

Xiuran Yin[1,2,3] · Weichao Wu[2,4,5] · Mara Maeke[1,3] · Tim Richter-Heitmann[1] · Ajinkya C. Kulkarni[1,2,3] · Oluwatobi E. Oni[1,2] · Jenny Wendt[2,4] · Marcus Elvert[2,4] · Michael W. Friedrich[1,2]

Received: 29 January 2019 / Revised: 4 April 2019 / Accepted: 13 April 2019 / Published online: 30 April 2019

Abstract

Methyl substrates are important compounds for methanogenesis in marine sediments but diversity and carbon utilization by methylotrophic methanogenic archaea have not been clarified. Here, we demonstrate that RNA-stable isotope probing (SIP) requires ^{13}C-labeled bicarbonate as co-substrate for identification of methylotrophic methanogens in sediment samples of the Helgoland mud area, North Sea. Using lipid-SIP, we found that methylotrophic methanogens incorporate 60–86% of dissolved inorganic carbon (DIC) into lipids, and thus considerably more than what can be predicted from known metabolic pathways (~40% contribution). In slurry experiments amended with the marine methylotroph *Methanococcoides methylutens*, up to 12% of methane was produced from CO_2, indicating that CO_2-dependent methanogenesis is an alternative methanogenic pathway and suggesting that obligate methylotrophic methanogens grow in fact mixotrophically on methyl compounds and DIC. Although methane formation from methanol is the primary pathway of methanogenesis, the observed high DIC incorporation into lipids is likely linked to CO_2-dependent methanogenesis, which was triggered when methane production rates were low. Since methylotrophic methanogenesis rates are much lower in marine sediments than under optimal conditions in pure culture, CO_2 conversion to methane is an important but previously overlooked methanogenic process in sediments for methylotrophic methanogens.

Introduction

Methanogenesis is the terminal step of organic matter mineralization in marine sediments [1]. There are three main pathways producing methane, i.e., hydrogenotrophic (H_2/CO_2), acetoclastic (acetate), and methylotrophic (e.g., methanol, methylamine, methoxylated benzoate) methanogenesis [2–4], with the former two pathways considered dominant. However, the importance of methylated compounds for methanogenesis in marine sediments has been acknowledged in recent years. Geochemical profiles and molecular analysis have shown that methylotrophic methanogenesis is the most significant pathway for methane formation in hypersaline sediments [5, 6] and in the sulfate reduction zone (SRZ) in marine environments [7, 8], where methanol concentration of up to 69 µM had been measured [9, 10]. Especially in the SRZ, methylated compounds are regarded as non-competitive substrates for methanogenesis, since sulfate reducing microorganisms apparently do not compete with methanogens for these compounds [11, 12]; in addition, methylated compounds can be used by marine homoacetogens [13]; however, in

These authors contributed equally: Xiuran Yin, Weichao Wu

Supplementary information The online version of this article (https://doi.org/10.1038/s41396-019-0425-9) contains supplementary material, which is available to authorized users.

✉ Michael W. Friedrich
michael.friedrich@uni-bremen.de

[1] Microbial Ecophysiology Group, Faculty of Biology/Chemistry, University of Bremen, Bremen, Germany

[2] MARUM - Center for Marine Environmental Sciences, Bremen, Germany

[3] International Max-Planck Research School for Marine Microbiology, Max Planck Institute for Marine Microbiology, Bremen, Germany

[4] Department of Geosciences, University of Bremen, Bremen, Germany

[5] Present address: Department of Biogeochemistry of Agroecosystems, University of Goettingen, Goettingen, Germany

marine sediments, evidence for this activity in competition with methanogens has not been obtained so far [14]. In sediments of the Helgoland mud area, specifically, high relative abundances of potential methylotrophic methanogens were observed [15] of which many are unknown. The potential for methylotrophic methanogenesis was recently even predicted from two metagenome-assembled genomes of uncultivated Bathyarchaeota, assembled from a shotgun metagenome [16].

The formation of methane via the three main pathways in methanogenic archaea has been studied intensively [17–19]. Much less is known regarding assimilation of carbon into biomass under in situ conditions and to which extent different carbon sources in the environment are utilized. Discrepancies between the predicted pathways known and the actual carbon metabolism measured appear to be based on (1) different cellular functions of carbon dissimilation and assimilation originated from reaction equilibria operative, (2) intermediate carbon cross utilization, and (3) interplay between different microbial communities [18, 20–23]. For example, mixotrophically growing cultures of *Methanosarcina barkeri* form their biomass equally from methanol and CO_2; however, almost all the methane is formed from methanol rather than from CO_2 since methanol is disproportionated to methane and CO_2 according to the following reaction:

$$4\ CH_3OH \rightarrow 3\ CH_4 + CO_2 + 2\ H_2O \quad (1)$$

But apart from such culture studies using the nutritionally versatile *M. barkeri*, the respective contribution of CO_2 and methylated carbon substrates to biomass formation during methylotrophic methanogenesis, especially for "obligate" methylotrophic methanogens, in natural sediments has not been studied to date.

Nucleic acids (RNA ~20%, DNA ~3%, of dry biomass, respectively), lipids (7–9%) and proteins (50–55%) are crucial cell components in living microorganisms [24], and thus, suitable markers of carbon assimilation. In order to characterize carbon assimilation capabilities, stable isotope probing (SIP) techniques exist, among which RNA-SIP is very powerful for identifying active microorganisms based on separating ^{13}C-labeled from unlabeled RNA using isopycnic centrifugation [25, 26]. In combination with downstream sequencing analysis, RNA-SIP provides high phylogenetic resolution in detecting transcriptionally active microbes [27, 28] but is limited in its sensitivity by requiring more than 10% of ^{13}C incorporation into RNA molecules for separating ^{13}C-labeled from unlabeled RNA [29]. To date, a number of SIP studies successfully detected methylotrophic bacteria [30–32] but the detection of methylotrophic methanogens by RNA-SIP with ^{13}C labeled methyl compounds might be hampered by mixotrophic growth [33].

In contrast to RNA-SIP, lipid-SIP has a lower phylogenetic resolution, but can detect very sensitively $\delta^{13}C$-values in lipid derivatives by gas chromatography combustion isotope ratio mass spectrometry (GC-c-IRMS), thereby facilitating quantitative determination of small amounts of assimilated carbon [34, 35].

In this study, we aimed to identify methylotrophic methanogens by RNA-SIP and elucidate carbon assimilation patterns in marine sediments. We hypothesized that the large pool of ambient dissolved inorganic carbon (DIC) in sediments [7] alters carbon utilization patterns in methylotrophic methanogens compared to pure cultures. To address this hypothesis, we tracked carbon dissimilation into methane and quantified assimilation into lipids by lipid-SIP in slurry incubations and pure cultures. In contrast to known pathways, we found a high degree of methane generation from DIC during methylotrophic methanogenesis by obligate methylotrophic methanogens, i.e., using only methyl groups for methane formation. This mixotrophic methanogenesis from both, methanol and DIC, might be the basis for our observation that more inorganic carbon was assimilated into biomass than could be expected from known pathways.

Materials and methods

Sediment incubation setup for SIP

Sediment was collected from the Helgoland mud area (54°05.23′N, 007°58.04′E) by gravity coring in 2015 during the RV HEINCKE cruise HE443. The geochemical profiles were previously described [15]. Sediments of the SRZ (16–41 cm) and MZ (238–263 cm) from gravity core HE443/077-1 were selected for incubations; typically, sulfate concentration for SRZ sediment is in the range of ~3–25 mM and for MZ sediment is below the detection threshold (~50 µM) as reported in Oni et al. [15]. Anoxic slurries (1:4; w/v) were prepared by mixing sediments with sterilized artificial sea water without sulfate [36]. Slurries of 50 mL were dispensed into sterile 120-mL serum bottles and sealed with butyl rubber stoppers. Residual oxygen was removed by exchanging bottle headspace three times with N_2 gas. A 10-day pre-incubation was performed, followed by applying vacuum (3 min at 100 mbar) to remove most of the headspace CO_2. Triplicate incubations were conducted by supplementing 1 mM ^{13}C-labeled methanol (~33 mg L^{-1} slurry) and unlabeled 10 mM sodium bicarbonate (~610 mg L^{-1} slurry), or 1 mM unlabeled methanol and 10 mM ^{13}C-labeled sodium bicarbonate (^{13}C-labeled substrates provided by Cambridge Isotope Laboratories, Tewksbury, MA, USA) at 10 °C. The proportion of ^{13}C DIC was determined by GC-c-IRMS.

Pure culture setup

The carbon assimilation patterns were compared between SIP sediment incubations and the obligate methylotrophic methanogen, *Methanococcoides methylutens*. *M. methylutens* strain MM1 (DSM 16625) was obtained from the German Collection of Microorganisms and Cell Cultures (DSMZ, Braunschweig, Germany). Initial cultivation was performed using medium 280 according to DSMZ protocols. After several transfers of the culture in anoxic marine Widdel medium [37], 5% of the culture were inoculated into fresh Widdel medium supplemented with 30 mM methanol, trace element solution SL 10 [38], and 50 mM sodium bicarbonate (i.e., DIC) with carbon sources containing 5% of ^{13}C-label. Pure cultures were grown at 30 °C in triplicates.

Slurry incubations inoculated with *M. methylutens*

To test methanogenesis from CO_2, incubations were performed with *M. methylutens* in autoclaved ($n = 3$) slurry from the SRZ with different amendments of electron donor (H_2), electron shuttles (humic acid; anthraquinone-2,6-disulfonic acid—AQDS), and electron acceptors/electron conductors (hematite, α-Fe_2O_3; magnetite, Fe_3O_4; Lanxess, Germany). Incubations were separately prepared with 50% H_2 in headspace, 100 µM AQDS, 30 mM magnetite, 30 mM hematite and 500 mg L^{-1} humic acid (Sigma-Aldrich, Steinheim, Germany). The pure culture (5%) was inoculated into these setups, and amended with 20 mM unlabeled methanol and ~10% of ^{13}C-labeled DIC (1 mM) for measuring carbon partitioning into methane. The control incubation comprised autoclaved slurry, 50% H_2 and 20 mM methanol without addition of *M. methylutens*. All experiments were set up with a total volume of 50 mL in 120-mL serum bottles sealed with butyl rubber stoppers, and incubated at 30 °C in triplicates.

Gas analysis

The concentration of methane in the headspace was measured by gas chromatography as previously described [39]. Headspace H_2 was determined with a reduction gas detector (Trace Analytical, Menlo Park, CA, USA). Gas samples of 100 µL and 1 mL from triplicate bottles were used for measuring methane and H_2, respectively. The parameters for H_2 measurement were as follows: carrier gas (nitrogen) 50 mL min^{-1}, injector temperature 110 °C, detector 230 °C, column (Porapak Q 80/100) 40 °C.

The δ^{13}C values of methane and CO_2 in the headspace, DIC as well as total inorganic carbon (TIC) in slurries were determined using a Thermo Finnigan Trace GC connected to a DELTA Plus XP IRMS (Thermo Scientific, Bremen, Germany) as described previously [40]. Prior to analyses of δ^{13}C-DIC and -TIC, 1 mL of supernatant or slurry was converted to CO_2 by adding 1 mL phosphoric acid (85%, H_3PO_4) overnight at room temperature.

Nucleic acids extraction, quantification, and DNase treatment

The nucleic acids were extracted according to Lueders et al. [41]. Briefly, 2 mL of wet sediment without supernatant from biological triplicates was used for cell lysis by bead beating, nucleic acid purification by phenol-chloroform-isoamyl alcohol extraction and precipitation with polyethylene glycol. For the RNA extract, DNA was removed by using the RQ1 DNase kit (Promega, Madison, WI, USA). DNA and RNA were quantified fluorimetrically using Quant-iT PicoGreen and Quant-iT RiboGreen (both Invitrogen, Eugene, OR, USA), respectively.

Isopycnic centrifugation, gradient fractionation, and reverse transcription

Isopycnic centrifugation and gradient fractionation were performed according to the previously described method with modifications [41]. In brief, 600–800 ng RNA from biological replicates ($n = 3$) was combined and loaded with 240 µL formamide, 6 mL cesium trifluoroacetate solution (CsTFA, GE Healthcare, Buckinghamshire, UK) and gradient buffer solution. RNA was density separated by centrifugation at 124,000 × g at 20 °C for 65 h using an Optima L-90 XP ultracentrifuge (Beckman Coulter, Brea, CA, USA). As standard, a mixture of equivalent amounts of fully ^{13}C-labeled and unlabeled *E. coli* RNA was used in density separation for defining heavy and light gradient fraction density ranges. RNA was quantified and reverse transcription was conducted using the high-capacity cDNA reverse transcription kit (Applied Biosystems, Foster City, CA, USA).

Quantitative PCR (qPCR)

Archaeal 16S rRNA and *mcrA* genes were quantified from each biological replicate ($n = 3$) using primer sets 806F/912R and ME2 mod/ME3′Fs 1011 (Table S1), respectively; *mcrA* encodes the alpha subunit of methyl coenzyme M reductase, a key enzyme of methanogenic and methanotrophic archaea [42]. Standard curves were based on the 16S rRNA gene of *M. barkeri* and the *mcrA* gene clone A4-67 for archaea and methanogens, respectively. The setup of PCR reaction was described previously [36]. The qPCR protocol comprised an initial denaturation for 5 min at 95 °C and 40 cycles amplification (95 °C for 30 s, 58 °C for 30 s, and 72 °C for 40 s). The detection thresholds were 100–1000 gene copies with an efficiency of 90–110%.

Sequencing and bioinformatics analysis

Based on the RNA-SIP profiles of *E.coli* standard RNA (Fig. S1) and previously reported density shifts in SIP fractions [41], "heavy" (1.803–1.823 g mL^{-1}, combination of fraction 3, 4, and 5) and "light" (1.777–1.780 g mL^{-1}, fraction 11) fractions of RNA-SIP samples were selected. Library construction and sequence read processing were as described previously [39].

Lipid analysis

Total lipids were extracted from ~4 g of freeze-dried sediment samples from single-labeling incubations (one substrate labeled, the other unlabeled) using a modified Bligh–Dyer protocol [43]. Intact polar archaeal ether lipids were purified by preparative high-performance liquid chromatography with fraction collection according to the method by Zhu et al. [44]. Considering the origin and complexity of sediment samples and similar proportion of carbon atoms in lipid molecules (archaeol (AR) and hydroxyarchaeol (OH-AR)), phytenes, biphytane, and biphytanes containing cycloalkyl rings (Figs. 3c and S2) were obtained from the intact archaeal lipid fraction [45]. The detailed chromatographic and mass spectrometric parameters were described by Kellermann et al. [46].

$\delta^{13}C$ calculation

The proportion of methane from DIC (f_{DIC/CH_4}) was calculated based on the fractional abundance of ^{13}C (^{13}F) of methane, methanol (MeOH) and DIC in the incubation with ^{13}C-DIC and MeOH. According to a two-end member model, DIC, and MeOH are two main carbon sources for methane production expressed as follows:

$$f_{DIC/CH_4}\,{}^{13}F_{DIC} + \left(1 - f_{DIC/CH_4}\right){}^{13}F_{MeOH} = {}^{13}F_{CH_4} \quad (2)$$

$$f_{DIC/CH_4} = \frac{{}^{13}F_{CH_4} - {}^{13}F_{MeOH}}{{}^{13}F_{DIC} - {}^{13}F_{MeOH}} \times 100\% \quad (3)$$

where ^{13}F is obtained from the δ notation according to $F = R/(1+R)$ and $R = (\delta/1000 + 1)$ * 0.011180 [47]. ${}^{13}F_{CH_4}$ and ${}^{13}F_{DIC}$ were the fractional ^{13}C abundance of methane and DIC at harvest time, and ${}^{13}F_{MeOH}$ that of MeOH in the medium at the start.

^{13}C label incorporation ratios from MeOH or DIC in single-labeling experiments were calculated from the ^{13}C abundance increase relative to the ^{13}C label strength via Eqs. (4) and (5). X_{MeOH} and X_{DIC} signify the ^{13}C incorporation ratio from MeOH and DIC, respectively. ${}^{13}F_{t_{end}}$ and ${}^{13}F_{t_0}$ are the ^{13}C fractional abundance of lipids harvested at t_{end} and t_0.

$$X_{MeOH} = \frac{{}^{13}F_{t_{end}} - {}^{13}F_{t_0}}{{}^{13}F_{MeOH}} \quad (4)$$

$$X_{DIC} = \frac{{}^{13}F_{t_{end}} - {}^{13}F_{t_0}}{{}^{13}F_{DIC}} \quad (5)$$

Given that the single-labeling incubations were conducted with the same treatment, i.e., 1 mM methanol and 10 mM DIC, the relative proportion of DIC for lipids biosynthesis ($f_{DIC/lipid}$) was estimated from the ^{13}C incorporation ratios (X_{MeOH} and X_{DIC}) in these single-labeling incubations as follow:

$$f_{DIC/lipid} = \frac{X_{DIC}}{X_{DIC} + X_{Me}} \quad (6)$$

Results

Methylotrophic methanogenesis and increase in methanogenic archaea

In order to examine carbon labeling into RNA and lipids of methylotrophic methanogens in anoxic marine environments, sediment slurries amended with or without ^{13}C-methanol (1 mM) and ^{13}C-DIC (10 mM) were incubated at 10 °C. Sediment incubations from the zones of sulfate reduction (SRZ) and methanogenesis (MZ) showed a divergent methane production rate, i.e., methanogenesis finished after 40 and 20 days, respectively (Fig. 1a). In incubations amended with DIC and ^{13}C-methanol, carbon recovery from methanol of ~80% was measured from both sediment incubations (Table S2). Amended ^{13}C-DIC was diluted into the sediment endogenous DIC pool to about 70–84%, which was more obvious in samples from MZ than SRZ (Table 1). In SRZ sediment incubations with ^{13}C-DIC and unlabeled methanol, up to 10.3% of methane originated from ^{13}C-DIC (Table 1).

The dynamics of the archaeal communities in all incubations was tracked by qPCR of archaeal 16S rRNA genes and *mcrA* genes after methanogenesis ceased (Fig. 1b). Archaeal and *mcrA* gene copy numbers increased strongly by 10–14 and 19–30 times for all treatment incubations, respectively, while gene copies in control incubations were not elevated (Fig. 1b).

Carbon assimilation into RNA and identification of metabolically active archaea

In preliminary sediment incubations, SIP experiments with ^{13}C-methanol had shown that RNA could not be labeled to a

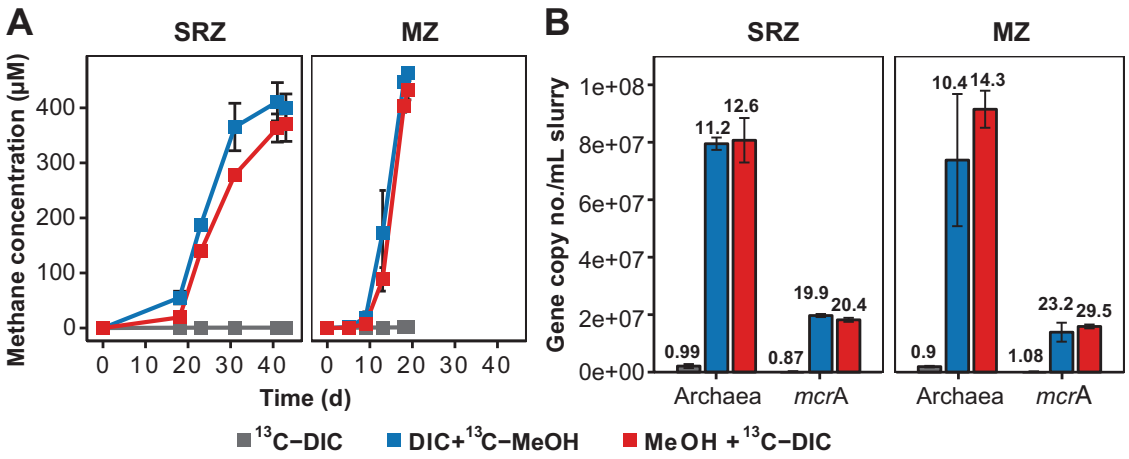

Fig. 1 Dynamics of methane formation and archaeal populations in stable isotope probing (SIP) incubations with SRZ and MZ sediment samples. **a** Methane concentrations in SIP incubations. Methane data are presented as average values ($n = 3$, error bar = SD). **b** Gene copy numbers of archaea (16S rRNA genes) and methanogens (*mcrA* gene). Gene copies were quantified based on DNA extracts at harvest. Fold increase of gene copies was indicated above each histogram by comparing gene copies on day 0 after pre-incubation ($n = 3$, error bar = SD). DIC dissolved inorganic carbon, i.e. bicarbonate; MeOH methanol

Table 1 ^{13}C fractional abundance and H_2 partial pressures in SIP incubations

Sediment	Substrates	$^{13}F_{DIC}$ (%)	f_{DIC/CH_4} (%)[a]	H_2 (Pa)[b]	Incubation time (d)
SRZ	DIC + ^{13}C-MeOH	3.7 ± 0.4	89.3 ± 0.3	NA	43
MZ	DIC + ^{13}C-MeOH	3.0 ± 0.0	96.4 ± 0.1	NA	19
SRZ	MeOH + ^{13}C-DIC	83.6 ± 0.6	10.3 ± 0.2	0.1 ± 0.1	43
MZ	MeOH + ^{13}C-DIC	69.8 ± 0.7	3.4 ± 0.1	0.3 ± 0.0	19

Data are presented as average values ($n = 3$)

NA not analyzed

[a]Methane proportion from DIC (f_{DIC/CH_4}) in "methanol+^{13}C-DIC" incubations was based on Eq. (3)

[b]H_2 partial pressure was measured on day 23 and 16 for incubation SRZ and MZ sediments, respectively

sufficiently high extent to become detectable in heavy gradient fractions (e.g., >1.803 g mL^{-1}) after isopycnic separation of RNA. Contrastingly, methanol dissimilation was strong and archaeal and *mcrA* gene copies increased compared to that on day 0 and ^{13}C-DIC control, likewise indicating that methylotrophic methanogens were active (Fig. 1a, b and Table S2). Because of mixotrophic assimilation capabilities in methylotrophic methanogens, i.e., utilizing methylated compounds and DIC, a series of SIP slurry experiments were conducted with combinations of methanol and DIC in order to improve the sensitivity of RNA-SIP: double ^{13}C-label (methanol+DIC), single ^{13}C-label (one of the substrates labeled), both substrates unlabeled, and a ^{13}C-DIC control (Figs. 2 and S3). After density separation of RNA, different degrees of RNA labeling were detected in isotopically heavy gradient fractions, e.g., >1.803 g mL^{-1} (Fig. 2). The strongest ^{13}C-labeling, as indicated by largest amounts of RNA found in gradient fractions >1.803 g mL^{-1}, was detected in RNA from incubations with double ^{13}C-labeling (Fig. 2a), followed by single-label incubations with ^{13}C-DIC. For single-label ^{13}C-methanol incubations, however, RNA fraction shifts according to density were minor compared to unlabeled incubations.

In order to estimate ^{13}C-labeling levels of methanogens in single SIP experiments (^{13}C-methanol or ^{13}C-DIC), a series of molecular techniques were applied including qPCR of cDNA in heavy fractions of RNA-SIP samples, archaeal 16S rRNA sequencing from RNA-SIP fractions and $\delta^{13}C$ value determination of methanogen lipids, e.g., phytanes derived from intact polar AR-based molecules. In incubations amended with ^{13}C-DIC and unlabeled methanol, archaeal gene copies were substantially higher than that of ^{13}C-DIC control and ^{13}C-methanol incubations (Fig. 2b). Up to 49,000-fold more RNA molecules were present in the heavy fraction (i.e., 1.803–1.823 g mL^{-1}) compared to the incubation amended with unlabeled DIC and ^{13}C-methanol (Table S3). Correspondingly, Illumina sequencing of RNA revealed that sequences identified as related to the genera *Methanococcoides* were dominant in SRZ sediment incubations, and the methylotrophic methanogens *Methanococcoides* and *Methanolobus* spp. were more dominant in MZ sediment incubations. In contrast to heavy fractions, the

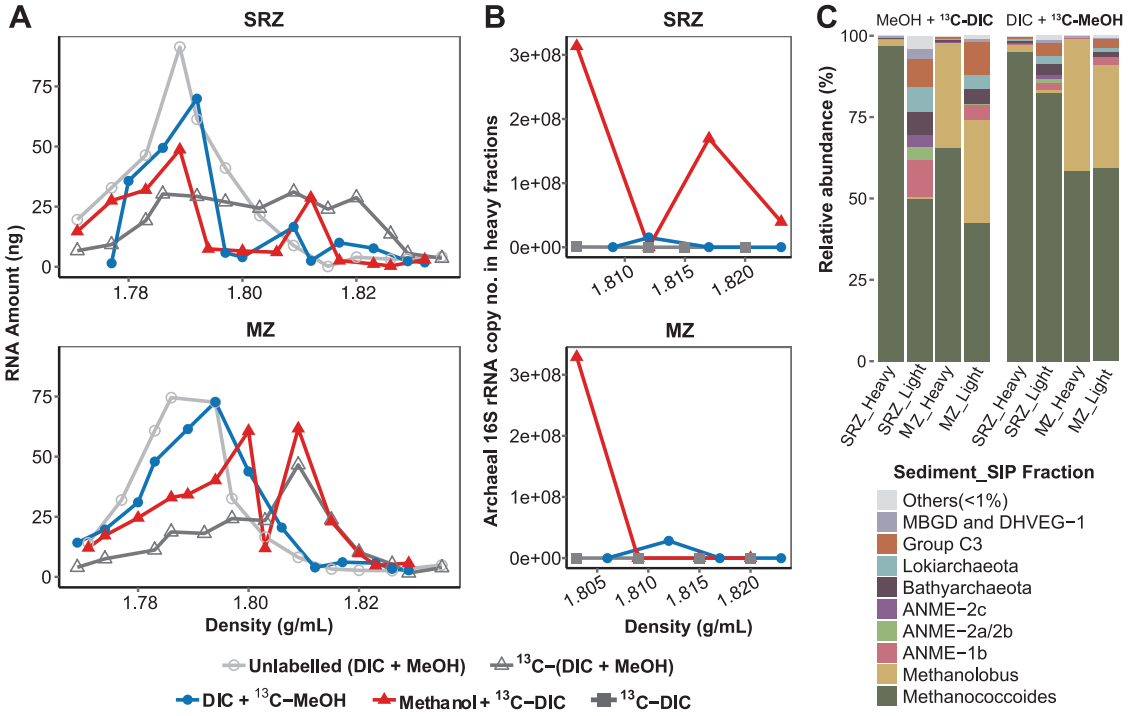

Fig. 2 Density distribution of RNA, gene copy numbers, and community composition from SIP incubations with SRZ and MZ sediment after isopycnic separation. **a** RNA profiles from different RNA-SIP experiments. **b** Gene copy numbers of archaeal cDNA in heavy fractions (1.803–1.823 g mL^{-1}) from RNA-SIP experiments. Archaeal gene copy numbers refer to the absolute abundance of 16S rRNA gene copies in cDNA from gradient fractions. **c** Relative abundances of density separated archaeal 16S rRNA from single-labeling incubations in light (1.771–1.800 g mL^{-1}) and heavy (1.803–1.835 g mL^{-1}) gradient fractions

abundance of methanogens in the light fractions from double labeling incubations, i.e., ^{13}C-(DIC + methanol), was lowest (~30–60%) (Fig. S3), followed by the incubations amended with methanol and ^{13}C-DIC (~50–70%) (Fig. 2c). SIP incubations amended with DIC and ^{13}C-methanol harbored the highest relative abundance of methanogens in the light fraction, which ranged in abundance from 80 to 90% of total archaea (Fig. 2c). Light fractions were overall mainly composed of anaerobic methanotrophic archaea, Bathyarchaeota, and Lokiarchaeota, except for methylotrophic methanogens (Fig. 2c). For ^{13}C-DIC control incubations, abundances of methanogens were low in SIP samples (Fig. S3). For unlabeled methanol and DIC incubations, given the low amount of labeled RNA in heavy fractions, no amplicons were obtained, but light fractions showed a high abundance of methylotrophic methanogens (Fig. S3). Classifications were confirmed by phylogenetic clustering of cloned 16S rRNA gene fragments (about 800 base pairs) with OTU sequences representing *Methanococcoides* and *Methanolobus* spp. (Fig. S4). Sequences of these methanogens accounted for more than 97% of total archaea in heavy gradient fractions. However, known hydrogenotrophic methanogens were undetectable (Fig. 2c), although 3 and 10% of methane was formed from DIC in incubations with MZ and SRZ sediments, respectively (Table 1).

In parallel to RNA-SIP, lipid-SIP incubations with SRZ sediment slurries demonstrated δ^{13}C values of phytane and phytenes being more positive in ^{13}C-DIC and unlabeled methanol treatment than that in ^{13}C-methanol amendments, while the opposite was found in MZ sediment incubations (Fig. 3a). After elimination of ^{13}C-DIC dilution effects by ambient inorganic carbon, DIC contributions to lipids ranged from 59.3 to 86.1% in SRZ sediment incubations, which was constantly higher than that of MZ sediment incubations (52.7–56.4%).

To understand how carbon is assimilated into lipids by methylotrophic methanogens, pure culture incubations of *M. methylutens* were performed with 5% of the ^{13}C-labeled substrates (i.e., DIC or MeOH) and the dominating archaeal lipids AR and OH-AR were directly analyzed without cleavage. In contrast to sediment incubations, lipids showed lower $f_{DIC/lipid}$ (~49%) based on the carbon incorporation in single-labeling incubations (Fig. 3b).

Methane formation from DIC during methylotrophic methanogenesis

The high proportion of methane formed from DIC in methanol amended sediment slurry incubations (Table 1) prompted us to investigate the underlying mechanism in

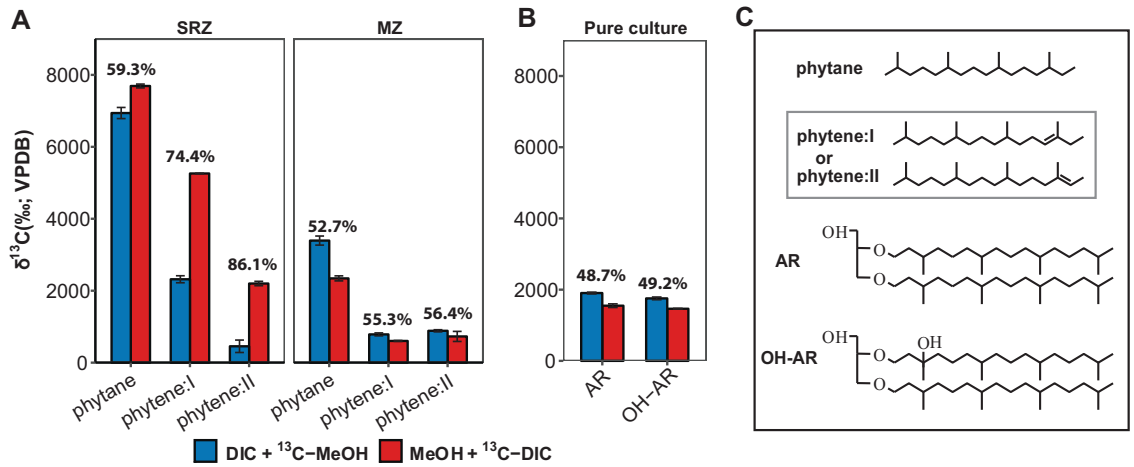

Fig. 3 Lipid-SIP experiments from sediment incubations (natural community) and pure cultures in Widdel medium. Lipid $\delta^{13}C$ values were measured in homogenized samples after methanogenesis had ceased. **a** $\delta^{13}C$ values of phytanes in sediment incubations with 70% ^{13}C-DIC. Phytane originates from intact polar archaeol lipids, phytenes (phytene I and phytene II) derive from intact polar hydroxyarchaeol lipids. $f_{DIC/lipid}$ are indicated on the top of bars from single-labeling incubations based on Eq. (6). **b** $\delta^{13}C$ values of archaeol (AR) and hydroxyarchaeol (AR-OH) in pure culture of *M. methylutens* treated with 5% ^{13}C-labeled substrates (methanol or DIC). **c** Structures of archaeal lipids. Enclosed structures of phytenes in (**c**) were tentatively assigned according to GC-MS mass spectra (Fig. S6) [80]. Data are expressed as average values ($n = 3$, error bar = SD)

more detail. Thus, autoclaved sediment slurries were used as a surrogate of natural sediment, but with all microorganisms killed, and inoculated with the obligate methylotroph *M. methylutens*. Hematite and magnetite known to serve as electron acceptors or conductors [48, 49] were added along with humic acid, and AQDS as electron shuttles, as well as an additional electron donor (H_2), which are all known to stimulate methanogenesis [48–51]; certain methylotrophic methanogens, e.g., *Methanomassiliicoccales* spp., require hydrogen for methanogenesis [52, 53].

Methane concentrations in incubations with hematite and humic acid were higher than that of the other incubations after 7 days (Fig. 4a). Although methane production rates were low, methane proportions from DIC in treatments with *M. methylutens* alone, H_2, AQDS and magnetite were much higher ($f_{DIC/CH4}$, ~10%) than that in incubations with hematite and humic acid (~2%) (Fig. 4b). Linear regression showed a strong correlation between methane production rate and CO_2-dependent methanogenesis by methylotrophic methanogens on day 3 and 5 of the incubations, indicating that lower methanogenesis rates triggered higher levels of methane formation derived from ^{13}C-DIC (Fig. 4c).

Discussion

In this study, we utilized RNA-SIP employing ^{13}C-DIC and methanol and successfully identified methylotrophic methanogens in both, SRZ and MZ sediments of the Helgoland mud area in the North Sea. We demonstrated that the addition of ^{13}C-DIC is necessary to detect label in RNA of methylotrophic methanogens rather than using ^{13}C-methanol as energy substrate alone. We further evaluated carbon utilization patterns of the methylotrophic methanogens by lipid-SIP and identified a high DIC assimilation into characteristic lipids within the SRZ sediment. Isotope probing experiments revealed that up to 12% of methane was formed from DIC by the "obligate" methylotrophic methanogen, *M. methylutens*, thereby suggesting an explanation for the elevated DIC incorporation into biomass.

Carbon assimilation by methylotrophic methanogens in sediment incubations

Nucleic acids-SIP techniques depend on ^{13}C-labeling levels of DNA or RNA molecules, from which carbon assimilation can be reconstructed and compared to the known pathway of nucleic acid biosynthesis from methyl groups in methanogens [54–59]. The current pathways show that only one carbon atom stems from methanol in ribose-5-phosphate while 25–40% of carbon in nucleobases originates from the methyl carbon of the substrate (Fig. 5). This is corroborated by our RNA-SIP experiments using ^{13}C-labeled methanol alone, but RNA was not found to be labeled effectively enough for density separation and further sequence analysis. However, by additionally using ^{13}C-DIC, we found high 16S rRNA copy numbers (Fig. 2b) and a high representation of known methylotrophic methanogens (Fig. 2c) in the heavy RNA gradient fractions, successfully recovering ^{13}C-labeled RNA of methylotrophic methanogens in the SRZ and MZ sediments of the Helgoland mud area. Combined

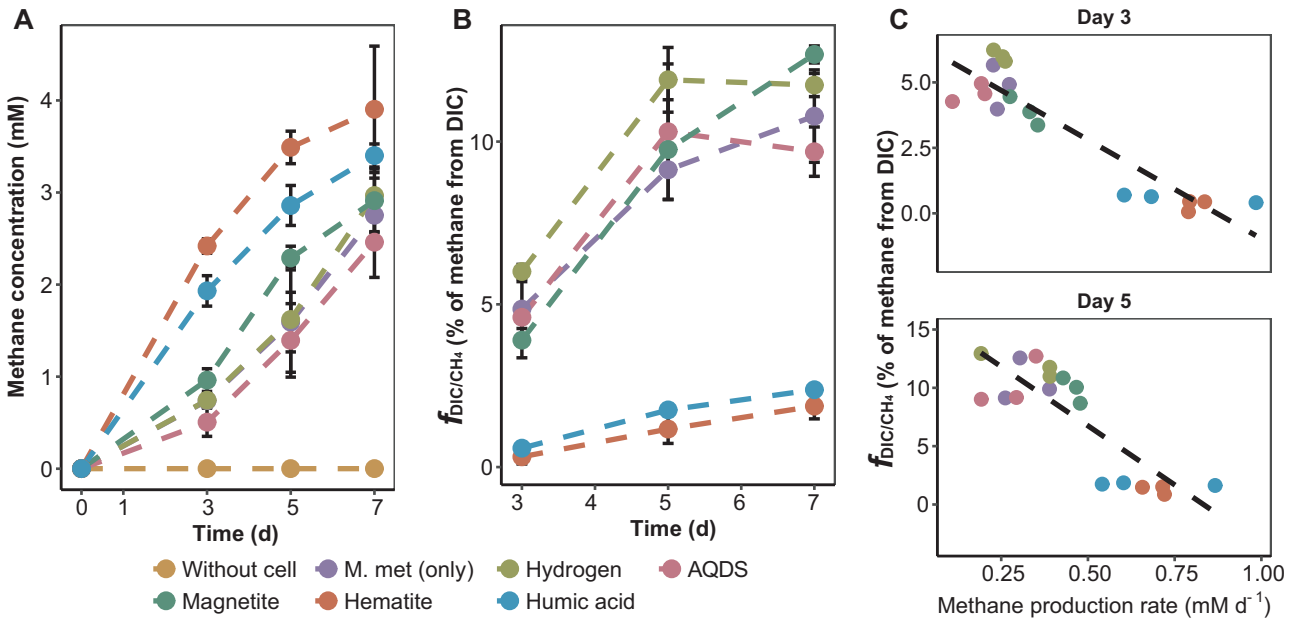

Fig. 4 Methane production from DIC during methylotrophic methanogenesis in autoclaved slurry supplemented with pure culture of *M. methylutens*. **a** Total methane concentrations in headspace. **b** Proportion of methane derived from DIC. Methane proportion from DIC (f_{DIC/CH_4}) was calculated according to Eq. (3). Data are expressed as average values ($n = 3$, error bar = SD). **c** Linear correlation between methanogenesis rate and methane proportion from DIC after 3 and 5 days. Day 3: Pearson's $r = -0.92$, $P < 0.001$, CI (0.95) = $-0.79 > r > -0.97$; Day 5: Pearson's $r = -0.85$, $P < 0.001$, CI (0.95) = $-0.62 > r > -0.94$

with downstream analysis including qPCR, 16S rRNA sequencing and cloning, we directly show that members of the genus *Methanococcoides* were the predominantly active methylotrophic methanogens in SRZ incubations, while *Methanococcoides* together with *Methanolobus* were dominant in MZ incubations. In addition, archaea with an abundance less than 0.01% showed a higher proportion in light fractions than in heavy fractions (Table S4), excluding the populations under high-sensitivity SIP conditions [60]. A small peak at 1.808 g mL^{-1} was detected in RNA-SIP profiles from the SRZ incubations amended with ^{13}C-methanol and unlabeled DIC, which originated most likely from methylotrophic methanogens as shown by relative abundances of methanogens in the heavy fractions (Fig. 2c). However, at this density, RNA was partially labeled only because of the lower contribution of methanol carbon to nucleic acid biosynthesis, which resulted in lower RNA amounts in heavy fractions than that of ^{13}C-DIC and unlabeled methanol treatment. Consequently, RNA labeling will be more effective in methylotrophic methanogenic archaea by using DIC than by methanol.

The main reactions of inorganic carbon assimilation are the generation of acetyl-CoA and pyruvate, respectively (Fig. 5). In principle, the generated CO_2 from methanol (Reaction 1) can be utilized for biomass synthesis but is in exchange with the large pool of ambient CO_2 (at least 10 mM in our experiments, up to 40 mM in marine sediment [7]. Thus, the methane formed by reduction of CO_2 will be largely recruited from ambient, unlabeled CO_2 molecules [61]. Hence, addition of ^{13}C-labeled DIC or a combination of both substrates labeled enables tracking of methylotrophic methanogens via RNA-SIP techniques. For carbon assimilation into nucleic acids of these methanogens, both proposed biosynthesis pathway of nucleic acid and labeling strategy of RNA-SIP confirmed inorganic carbon as the main carbon source for nucleic acids.

Because of its proven accuracy, lipid-SIP was used for the relative quantification of carbon assimilation into biomass. In lipid-SIP analysis, we evaluated ^{13}C-incorporation into intact polar AR- and OH-AR diether molecules, which are the dominant lipids produced by moderately thermophilic methanogenic archaea [62–64], via phytane and phytene side-chain analysis (Fig. 3). These moieties were the only ones being ^{13}C-labeled while tetraether-derived biphytane and cycloalkylated biphytanes as indicators of archaea such as Thaumarchaeota [65], anaerobic methanotrophs [66, 67] or Bathyarchaeota [68] did not show a ^{13}C incorporation (Fig. S5). This was corroborated by our sequencing results demonstrating that methylotrophic methanogens were the dominant archaea in the heavy fractions and that the relative abundances of other archaea were very low or even below detection (Fig. 2c).

By evaluating ^{13}C incorporation into methanogen-derived phytane and phytenes, lipid-SIP provides insight into methanogen activities and carbon utilization. As the main precursors of ether lipids in archaea, biosynthesis of

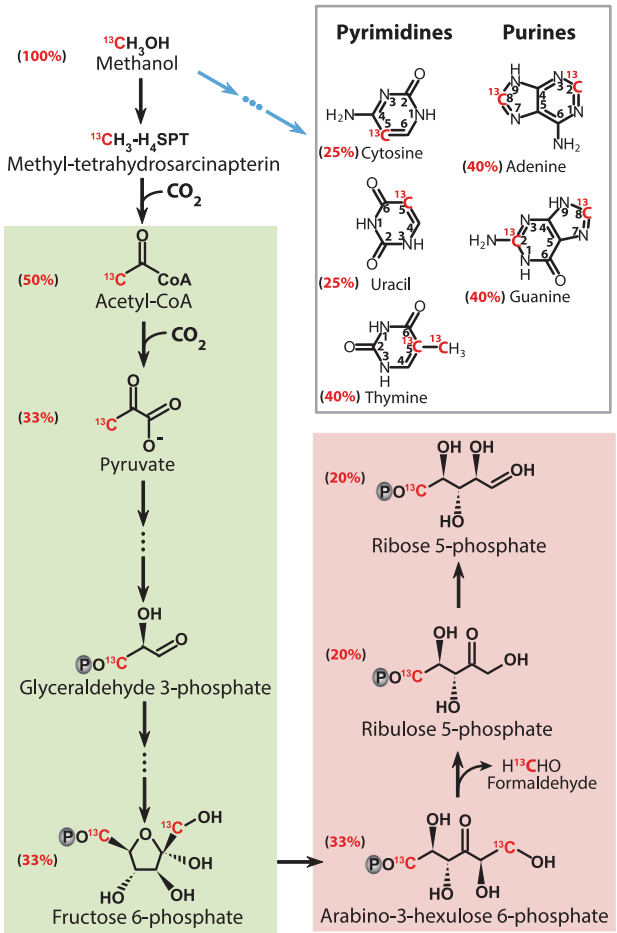

Fig. 5 Biosynthesis of nucleotide moieties, the pyrimidine and purine bases, as well as the C5-carbon from ^{13}C-labeled methanol in methylotrophic methanogens based on previous studies [54–59] with final carbon contribution from methanol added besides the compounds. Black arrows indicate ribose synthesis and the blue arrows represent synthesis of base moieties in nucleosides. The reverse gluconeogenesis pathway is displayed in green and the reverse ribulose monophosphate pathway in pink

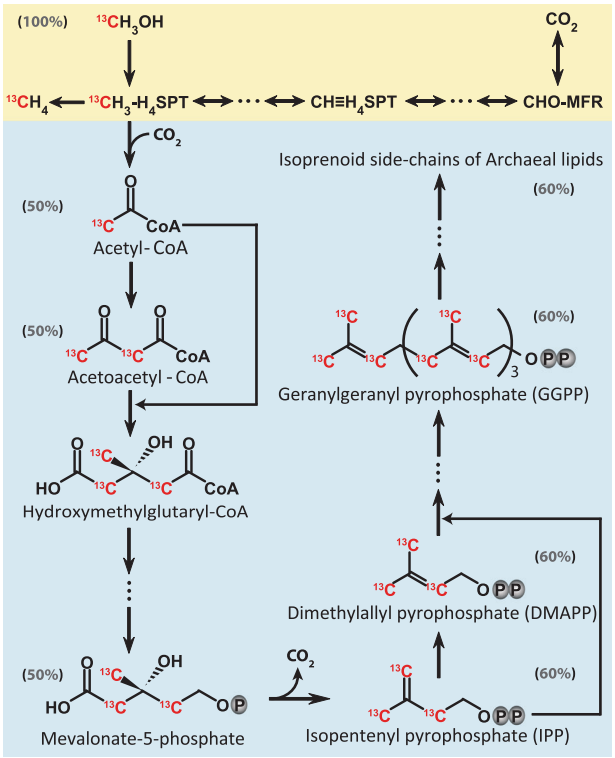

Fig. 6 Methylotrophic methanogenesis pathway from methanol (yellow) and carbon assimilation pattern into isoprenoid chains of archaeal lipids (blue) with carbon contribution from ^{13}C-methanol added besides the compounds. The pathway of archaeal lipid biosynthesis is based on previous studies [69, 81, 82]

isopentenyl diphosphate (IPP) and dimethylallyl diphosphate (DMAPP) proceeds via the modified mevalonate pathway [69–71]. In this pathway, mevalonate-5-phosphate is decarboxylated to IPP, in which three out of five carbon atoms are derived from methanol (Fig. 6). DMAPP is further converted to geranylgeranyl diphosphate, which receives 60% of its carbon from methanol, suggestive of a lower DIC contribution to isoprenoid chains than methanol. This was supported by the fact that AR and OH-AR contained more methanol-derived than DIC-derived carbon using a pure culture of *M. methylutens* (Fig. 3b). However, unlike the proposed lipid biosynthesis pathway and the pure culture, clearly more DIC was assimilated into lipids than methanol in both sediment incubations, which was most prominent in the sediment from the SRZ (Fig. 3a). We, moreover, detected that ~10% of methane produced was derived from DIC during the SIP experiments and using *M. methylutens* in autoclaved sediment slurry incubations (Table 1 and Fig. 4). Because of the reversibility of all reactions from CO_2 to methyl-tetrahydrosarcinapterin (CH_3-H_4SPT) [23], it is very likely that part of the DIC is converted to CH_3-H_4SPT. Thus, CH_3-H_4SPT generated from CO_2 will be available for lipid biosynthesis (Fig. 6) leading to the ^{13}C-enrichment of the lipid pool observed (Fig. 3).

CO_2 reduction to methane by obligate methylotrophic methanogens

There are two types of CO_2-dependent methanogenesis: (1) Hydrogenotrophic methanogenesis [2, 4]. These methanogens contain F_{420}-reducing [NiFe]-hydrogenase to catalyze F_{420} reduction by H_2 [72]. (2) Mediation by interspecies electron transfer between bacteria and some members of the *Methanosarcinales*. CO_2 reduction to methane was observed in *Methanosaeta* and *Methanosarcina* during syntrophic growth with *Geobacter* species on alcohols (ethanol, propanol, and butanol), as electrons generated from *Geobacter* are directly transferred to methanogens to reduce CO_2 [73–76].

Based on our SIP incubations with SRZ sediment showing 10% of methane generation from DIC at low H_2 partial pressure (<0.3 Pa) (Table 1) and the overall lack of hydrogenotrophic methanogens in RNA-SIP fractions (Fig. 2c), we argue that H_2-dependent methanogenesis does not play a role [2]. Similarly, in autoclaved sediment slurry (Fig. 4b), the "obligate" methylotroph *M. methylutens* generated methane from CO_2 without a hydrogen (or electron) supplying partner microorganism.

Members of the genus *Methanococcoides* are considered as obligate methylotrophic methanogens since no F_{420}-reducing [NiFe]-hydrogenase was detected in their genomes [69, 77] ruling out hydrogenotrophic methanogenesis in sediment incubations. Nevertheless, part of the methane formed during methylotrophic methanogenesis by *M. methylutens* was from CO_2, especially when methane production rates were low (Fig. 4c). Apparently, at high rates of methanol dissimilation to CO_2, the reverse pathway of CO_2 reduction to methane was outcompeted. Higher rates of methylotrophic methanogenesis can be achieved potentially by amendments in autoclaved slurries using hydrogen as electron donor, electron conductors (hematite, magnetite) and electron shuttles (humic acid, AQDS); in our incubations, we found humic acid and hematite most strongly stimulating methylotrophic methanogenesis. Although the underlying mechanism is beyond the scope of the current study, methylotrophic methanogens in our incubations could take advantage of hematite as potential electron conductor [48, 49] or humic acid as electron shuttle [51] as indicated by a higher rate of methanogenesis compared to the other treatments (Fig. 4a).

It has been shown that 3% of methane was produced from CO_2 during methylotrophic methanogenesis of *M. barkeri* (i.e., a facultative methylotroph) without the addition of H_2 [33], which is similar to about 2.5% of methane generated from CO_2 by *M. methylutens* (i.e., "obligate" methylotroph) in our study (Table S5). However, in SRZ sediment incubations the rate of methane production was lower than in MZ incubations, which resulted in a high proportion of methane generated from CO_2 (10%) (Table 1 and Fig. 1). Furthermore, CO_2 conversion to methane linked inorganic carbon assimilation into lipids, highlighting the importance of the activity of concomitant CO_2 reduction during methylotrophic methanogenesis in marine sediments. In contrast, we found that in pure cultures, under optimal growth conditions, a substantially higher methanogenesis rate decreases the amount of methane produced from CO_2. In marine sediment methylotrophic methanogenesis rates are likely lower than those in pure cultures because of the limitation in methylated substrates [7, 18], strongly suggesting that methane generation from CO_2 by obligate methylotrophic methanogens is underestimated under in situ conditions. Thus, CO_2 conversion to methane has to be considered when estimates of in situ methylotrophic methanogenesis in marine sediments are performed.

In summary, we have shown that ^{13}C-DIC is required as cosubstrate for successful identification of methylotrophic methanogens by RNA-SIP in marine sediments. DIC is the main carbon source for biosynthesis of nucleic acids in these methanogens and thus using ^{13}C-methanol as energy and carbon substrate alone is insufficient in SIP experiments (Fig. 5). Given the intricacies of known assimilatory pathways in methanogenic archaea as a functional group, it might be necessary to at least check for the possibility of DIC as a main assimilatory carbon component in all methanogens for successful SIP experiments. In general, it seems that archaea have a propensity for using DIC as a carbon source for assimilation [68, 78], possibly as an evolutionary adaptation to environments with limited availability of organic carbon [79].

But beyond known pathways, we detected an unexpectedly high amount of methane (>10%) formed from DIC. Especially in SRZ incubations, the lower methane production rates resulted in increased CO_2 conversion to methane (~10%), which is linked to CO_2 assimilation. This finding strongly suggests that the alleged obligate methylotroph studied here was rather mixotrophically converting both available substrates (DIC, methanol) to methane. Our detailed labeling studies showed that the kinetics of substrate utilization apparently is a decisive factor in channeling more or less CO_2 into the pathway of methanogenesis: more methane formed from CO_2 when the overall kinetics were slow, and vice versa. From an ecological perspective, DIC is a much more pertinent substrate than methanol (or other methyl compounds) in marine sediments [5, 7], and thus we speculate that more DIC reduction by obligate methylotrophic methanogens occurs in situ than is currently known. A larger proportion of methane formed from DIC in methylotrophic methanogens should also impact interpretation of $\delta^{13}CH_4$ values and associated carbon isotope fractionations, which might be overprinted by such mixotrophic methanogenesis. Thus, the CO_2 reduction to methane and assimilation into biomass by obligate methylotrophic methanogens plays a much more important role in the environment than was previously known.

Data availability

Sequencing data have been submitted to GenBank Short Reads Archive with accession numbers from SRR8207425 to SRR8207442.

Acknowledgements This study was supported by the Research Center/Cluster of Excellence EXC 309 (project-ID 49926684) 'The Ocean in the Earth System' and the Cluster of Excellence EXC 2077 (project-ID 390741601) 'The Ocean Floor – Earth's Uncharted Interface' funded by the Deutsche Forschungsgemeinschaft (DFG) and by

the University of Bremen. Xiuran Yin and Weichao Wu were additionally funded by scholarships from China Scholarship Council (CSC). We thank the captain, crew and scientists of R/V HEINCKE expeditions HE443.

Compliance with ethical standards

Conflict of interest The authors declare that they have no conflict of interest.

Publisher's note: Springer Nature remains neutral with regard to jurisdictional claims in published maps and institutional affiliations.

References

1. Ferry JG, Lessner DJ. Methanogenesis in marine sediments. Ann N Y Acad Sci. 2008;1125:147–57.
2. Thauer RK, Kaster AK, Seedorf H, Buckel W, Hedderich R. Methanogenic archaea: ecologically relevant differences in energy conservation. Nat Rev Microbiol. 2008;6:579–91.
3. Mayumi D, Mochimaru H, Tamaki H, Yamamoto K, Yoshioka H, Suzuki Y, et al. Methane production from coal by a single methanogen. Science. 2016;235:222–5.
4. Liu Y, Whitman WB. Metabolic, phylogenetic, and ecological diversity of the methanogenic archaea. Ann N Y Acad Sci. 2008;1125:171–89.
5. Zhuang G-C, Elling FJ, Nigro LM, Samarkin V, Joye SB, Teske A, et al. Multiple evidence for methylotrophic methanogenesis as the dominant methanogenic pathway in hypersaline sediments from the Orca Basin, Gulf of Mexico. Geochim Cosmochim Acta. 2016;187:1–20.
6. Lazar CS, Parkes RJ, Cragg BA, L'Haridon S, Toffin L. Methanogenic diversity and activity in hypersaline sediments of the centre of the Napoli mud volcano, Eastern Mediterranean Sea. Environ Microbiol. 2011;13:2078–91.
7. Zhuang G-C, Heuer VB, Lazar CS, Goldhammer T, Wendt J, Samarkin VA, et al. Relative importance of methylotrophic methanogenesis in sediments of the Western Mediterranean Sea. Geochim Cosmochim Acta. 2018;224:171–86.
8. Maltby J, Steinle L, Löscher CR, Bange HW, Fischer MA, Schmidt M, et al. Microbial methanogenesis in the sulfate-reducing zone of sediments in the Eckernförde Bay, SW Baltic Sea. Biogeosciences. 2018;15:137–57.
9. Yanagawa K, Tani A, Yamamoto N, Hachikubo A, Kano A, Matsumoto R, et al. Biogeochemical cycle of methanol in anoxic deep-sea sediments. Microbes Environ. 2016;31:190–3.
10. Zhuang G-C, Lin Y-S, Elvert M, Heuer VB, Hinrichs K-U. Gas chromatographic analysis of methanol and ethanol in marine sediment pore waters: validation and implementation of three pretreatment techniques. Mar Chem. 2014;160:82–90.
11. Oremland RS, Polcin S. Methanogenesis and sulfate reduction: competitive and noncompetitive substrates in estuarine sediments. Appl Environ Microbiol. 1982;44:1270–6.
12. Florencio L, Field JA, Lettinga G. Importance of cobalt for individual trophic groups in an anaerobic methanol-degrading consortium. Appl Environ Microbiol. 1994;60:227–34.
13. Balch WE, Schoberth S, Tanner RS, Wolfe RS. *Acetobacterium*, a new genus of hydrogen-oxidizing, carbon dioxide-reducing, anaerobic bacteria. Int J Syst Evol Microbiol. 1977;27:355–61.
14. Lever MA. Acetogenesis in the energy-starved deep biosphere - a paradox? Front Microbiol. 2012;2:284.
15. Oni O, Miyatake T, Kasten S, Richter-Heitmann T, Fischer D, Wagenknecht L, et al. Distinct microbial populations are tightly linked to the profile of dissolved iron in the methanic sediments of the Helgoland mud area, North Sea. Front Microbiol. 2015;6:365.
16. Evans PN, Parks DH, Chadwick GL, Robbins SJ, Orphan VJ, Golding SD, et al. Methane metabolism in the archaeal phylum Bathyarchaeota revealed by genome-centric metagenomics. Science. 2015;350:432–8.
17. Weimer PJ, Zeikus JG. Acetate metabolism in *Methanosarcina barkeri*. Arch Microbiol. 1978;119:175–82.
18. Summons RE, Franzmann PD, Nichols PD. Carbon isotopic fractionation associated with methylotrophic methanogenesis. Org Geochem. 1998;28:465–75.
19. Hippe H, Caspari D, Fiebig K, Gottschalk G. Utilization of trimethylamine and other N-methyl compounds for growth and methane formation by *Methanosarcina barkeri*. Proc Natl Acad Sci USA. 1979;76:494–8.
20. Teeling H, Glockner FO. Current opportunities and challenges in microbial metagenome analysis—a bioinformatic perspective. Brief Bioinform. 2012;13:728–42.
21. Singer E, Wagner M, Woyke T. Capturing the genetic makeup of the active microbiome in situ. ISME J. 2017;11:1949–63.
22. Neelakanta G, Sultana H. The use of metagenomic approaches to analyze changes in microbial communities. Microbiol Insights. 2013;6:37–48.
23. Thauer RK. Anaerobic oxidation of methane with sulfate: on the reversibility of the reactions that are catalyzed by enzymes also involved in methanogenesis from CO_2. Curr Opin Microbiol. 2011;14:292–9.
24. Feijo Delgado F, Cermak N, Hecht VC, Son S, Li Y, Knudsen SM, et al. Intracellular water exchange for measuring the dry mass, water mass and changes in chemical composition of living cells. PLoS ONE. 2013;8:e67590.
25. Friedrich MW. Stable-isotope probing of DNA: insights into the function of uncultivated microorganisms from isotopically labeled metagenomes. Curr Opin Biotechnol. 2006;17:59–66.
26. Lueders T. Stable isotope probing of hydrocarbon-degraders. In: McGenity TJ, Timmis KN, Nogales B (eds). Handbook of hydrocarbon and lipid microbiology. Springer: Berlin, Heidelberg, 2010, pp 4011–26.
27. Grob C, Taubert M, Howat AM, Burns OJ, Dixon JL, Richnow HH, et al. Combining metagenomics with metaproteomics and stable isotope probing reveals metabolic pathways used by a naturally occurring marine methylotroph. Environ Microbiol. 2015;17:4007–18.
28. Fortunato CS, Huber JA. Coupled RNA-SIP and metatranscriptomics of active chemolithoautotrophic communities at a deep-sea hydrothermal vent. ISME J. 2016;10:1925–38.
29. Manefield M, Whiteley AS, Ostle N, Ineson P, Bailey MJ. Technical considerations for RNA- based stable isotope probing an approach to associating microbial diversity with microbial community function. Rapid Commun Mass Spectrom. 2002;16:2179–83.
30. Vandieken V, Thamdrup B. Identification of acetate-oxidizing bacteria in a coastal marine surface sediment by RNA-stable

isotope probing in anoxic slurries and intact cores. FEMS Microbiol Ecol. 2013;84:373–86.
31. Lueders T, Wagner B, Claus P, Friedrich MW. Stable isotope probing of rRNA and DNA reveals a dynamic methylotroph community and trophic interactions with fungi and protozoa in oxic rice field soil. Environ Microbiol. 2003;6:60–72.
32. Neufeld JD, Schafer H, Cox MJ, Boden R, McDonald IR, Murrell JC. Stable-isotope probing implicates *Methylophaga* spp and novel *Gammaproteobacteria* in marine methanol and methylamine metabolism. ISME J. 2007;1:480–91.
33. Weimer PJ, Zeikus JG. One carbon metabolism in methanogenic bacteria. Arch Microbiol. 1978;119:47–57.
34. Wegener G, Kellermann MY, Elvert M. Tracking activity and function of microorganisms by stable isotope probing of membrane lipids. Curr Opin Biotechnol. 2016;41:43–52.
35. Boschker HTS, Nold SC, Wellsbury P, Bos D, de Graaf W, Pel R, et al. Direct linking of microbial populations to specific biogeochemical processes by ^{13}C-labelling of biomarkers. Nature. 1998; 392:801–5.
36. Reyes C, Schneider D, Thürmer A, Kulkarni A, Lipka M, Sztejrenszus SY, et al. Potentially active iron, sulfur, and sulfate reducing bacteria in skagerrak and bothnian bay sediments. Geomicrobiol J. 2017;34:840–50.
37. Widdel F, Pfennig N. Studies on dissimilatory sulfate-reducing bacteria that decompose fatty acids I. Isolation of new sulfate-reducing bacteria enriched with acetate from saline environments. Description of *Desulfobacter postgateigen*. nov., sp. nov. Arch Microbiol. 1981;134:282–5.
38. Widdel F, Kohring GW, Mayer F. Studies on dissimilatory sulfate-reducing bacteria that decompose fatty acids III. Characterization of the filamentous gliding *Desulfonema limicola* gen. nov. sp. nov., and *Desulfonema magnum* sp. nov. Arch Microbiol. 1983;134:286–94.
39. Aromokeye DA, Richter-Heitmann T, Oni OE, Kulkarni A, Yin X, Kasten S, et al. Temperature controls crystalline iron oxide utilization by microbial communities in methanic ferruginous marine sediment incubations. Front Microbiol. 2018;9:2574.
40. Ertefai TF, Heuer VB, Prieto-Mollar X, Vogt C, Sylva SP, Seewald J, et al. The biogeochemistry of sorbed methane in marine sediments. Geochim Cosmochim Acta. 2010;74:6033–48.
41. Lueders T, Manefield M, Friedrich MW. Enhanced sensitivity of DNA- and rRNA-based stable isotope probing by fractionation and quantitative analysis of isopycnic centrifugation gradients. Environ Microbiol. 2004;6:73–8.
42. Friedrich MW. Methyl-coenzyme M reductase genes: unique functional markers for methanogenic and anaerobic methane-oxidizing Archaea. Methods Enzymol. 2005;397:428–42.
43. Sturt HF, Summons RE, Smith K, Elvert M, Hinrichs KU. Intact polar membrane lipids in prokaryotes and sediments deciphered by high-performance liquid chromatography/electrospray ionization multistage mass spectrometry—new biomarkers for biogeochemistry and microbial ecology. Rapid Commun Mass Spectrom. 2004;18:617–28.
44. Zhu C, Lipp JS, Wörmer L, Becker KW, Schröder J, Hinrichs K-U. Comprehensive glycerol ether lipid fingerprints through a novel reversed phase liquid chromatography–mass spectrometry protocol. Org Geochem. 2013;65:53–62.
45. Liu X-L, Lipp JS, Simpson JH, Lin Y-S, Summons RE, Hinrichs K-U. Mono- and dihydroxyl glycerol dibiphytanyl glycerol tetraethers in marine sediments: Identification of both core and intact polar lipid forms. Geochim Cosmochim Acta. 2012;89:102–15.
46. Kellermann MY, Yoshinaga MY, Wegener G, Krukenberg V, Hinrichs K-U. Tracing the production and fate of individual archaeal intact polar lipids using stable isotope probing. Org Geochem. 2016;95:13–20.
47. Boschker HTS, Middelburg JJ. Stable isotopes and biomarkers in microbial ecology. FEMS Microbiol Ecol. 2002;40:85–95.
48. Kato S, Hashimoto K, Watanabe K. Methanogenesis facilitated by electric syntrophy via (semi)conductive iron-oxide minerals. Environ Microbiol. 2012;14:1646–54.
49. Kato S, Nakamura R, Kai F, Watanabe K, Hashimoto K. Respiratory interactions of soil bacteria with (semi)conductive iron-oxide minerals. Environ Microbiol. 2010;12:3114–23.
50. Bond DR, Lovley DR. Reduction of Fe(III) oxide by methanogens in the presence and absence of extracellular quinones. Environ Microbiol. 2002;4:115–24.
51. Lovley DR, Fraga JL, Coates JD, Blunt-Harris EL. Humics as an electron donor for anaerobic respiration. Environ Microbiol. 1999;1:89–99.
52. Borrel G, Harris HM, Tottey W, Mihajlovski A, Parisot N, Peyretaillade E, et al. Genome sequence of "*Candidatus* Methanomethylophilus alvus" Mx1201, a methanogenic archaeon from the human gut belonging to a seventh order of methanogens. J Bacteriol. 2012;194:6944–5.
53. Borrel G, O'Toole PW, Harris HM, Peyret P, Brugere JF, Gribaldo S. Phylogenomic data support a seventh order of methylotrophic methanogens and provide insights into the evolution of methanogenesis. Genome Biol Evol. 2013;5:1769–80.
54. Choquet CG, Richards JC, Patel GB, Sprott GD. Ribose biosynthesis in methanogenic bacteria. Arch Microbiol. 1994a;161: 481–8.
55. Choquet CG, Richards JC, Patel GB, Sprott GD. Purine and pyrimidine biosynthesis in methanogenic bacteria. Arch Microbiol. 1994b;161:471–80.
56. Ekiel I, Smith ICP, Sportt GD. Biosynthetic pathways in *Methanospirillum hungatei* as determined by ^{13}C nuclear magnetic resonance. J Bacteriol. 1983;156:316–26.
57. Nyce GW, White RH. dTMP biosynthesis in archaea. J Bacteriol. 1996;178:914–6.
58. Soderberg T. Biosynthesis of ribose-5-phosphate and erythrose-4-phosphate in archaea: a phylogenetic analysis of archaeal genomes. Archaea. 2005;1:347–52.
59. Sorokin DY, Makarova KS, Abbas B, Ferrer M, Golyshin PN, Galinski EA, et al. Discovery of extremely halophilic, methyl-reducing euryarchaea provides insights into the evolutionary origin of methanogenesis. Nat Microbiol. 2017;2:17081.
60. Aoyagi T, Morishita F, Sugiyama Y, Ichikawa D, Mayumi D, Kikuchi Y, et al. Identification of active and taxonomically diverse 1,4-dioxane degraders in a full-scale activated sludge system by high-sensitivity stable isotope probing. ISME J. 2018;12:2376–88.
61. Wegener G, Niemann H, Elvert M, Hinrichs KU, Boetius A. Assimilation of methane and inorganic carbon by microbial communities mediating the anaerobic oxidation of methane. Environ Microbiol. 2008;10:2287–98.
62. Nishihara M, Koga Y. Hydroxyarchaetidylserine and hydroxyarchaetidyl-myo-inositol in *Methanosarcina barkeri*: polar lipids with a new ether core portion. Biochim Biophys Acta. 1991;1082:211–7.
63. Nishihara M, Utagawa M, Akutsu H, Koga Y. Archaea contain a novel diether phosphoglycolipid with a polar head group identical to the conserved core of eucaryal glycosyl phosphatidylinosito. J Biol Chem. 1992;267:12432–5.
64. Pancost RD, McClymont EL, Bingham EM, Roberts Z, Charman DJ, Hornibrook ERC, et al. Archaeol as a methanogen biomarker in ombrotrophic bogs. Org Geochem. 2011;42:1279–87.
65. Elling FJ, Könneke M, Lipp JS, Becker KW, Gagen EJ, Hinrichs K-U. Effects of growth phase on the membrane lipid composition of the thaumarchaeon *Nitrosopumilus maritimus* and their implications for archaeal lipid distributions in the marine environment. Geochim Cosmochim Acta. 2014;141:579–97.

66. Blumenberg M, Seifert R, Reitner J, Pape T, Michaelis W. Membrane lipid patterns typify distinct anaerobic methanotrophic consortia. Proc Natl Acad Sci USA. 2004;101:11111–6.
67. Rossel PE, Lipp JS, Fredricks HF, Arnds J, Boetius A, Elvert M, et al. Intact polar lipids of anaerobic methanotrophic archaea and associated bacteria. Org Geochem. 2008;39:992–9.
68. Yu T, Wu W, Liang W, Lever MA, Hinrichs KU, Wang F. Growth of sedimentary Bathyarchaeota on lignin as an energy source. Proc Natl Acad Sci USA. 2018;115:6022–7.
69. Allen MA, Lauro FM, Williams TJ, Burg D, Siddiqui KS, De Francisci D, et al. The genome sequence of the psychrophilic archaeon, *Methanococcoides burtonii*: the role of genome evolution in cold adaptation. ISME J. 2009;3:1012–35.
70. Grochowski LL, Xu H, White RH. *Methanocaldococcus jannaschii* uses a modified mevalonate pathway for biosynthesis of isopentenyl diphosphate. J Bacteriol. 2006;188:3192–8.
71. Nichols DS, Miller MR, Davies NW, Goodchild A, Raftery M, Cavicchioli R. Cold adaptation in the Antarctic archaeon *Methanococcoides burtonii* involves membrane lipid unsaturation. J Bacteriol. 2004;186:8508–15.
72. Thauer RK, Kaster AK, Goenrich M, Schick M, Hiromoto T, Shima S. Hydrogenases from methanogenic archaea, nickel, a novel cofactor, and H_2 storage. Annu Rev Biochem. 2010;79:507–36.
73. Lovley DR. Happy together: microbial communities that hook up to swap electrons. ISME J. 2017;11:327–36.
74. Rotaru AE, Shrestha PM, Liu F, Markovaite B, Chen S, Nevin KP, et al. Direct interspecies electron transfer between *Geobacter metallireducens*and *Methanosarcina barkeri*. Appl Environ Microbiol. 2014;80:4599–605.
75. Rotaru A-E, Shrestha PM, Liu F, Shrestha M, Shrestha D, Embree M, et al. A new model for electron flow during anaerobic digestion: direct interspecies electron transfer to *Methanosaeta* for the reduction of carbon dioxide to methane. Energy Environ Sci. 2014;7:408–15.
76. Wang LY, Nevin KP, Woodard TL, Mu BZ, Lovley DR. Expanding the diet for DIET: electron donors supporting direct interspecies electron transfer (DIET) in defined co-cultures. Front Microbiol. 2016;7:236.
77. Guan Y, Ngugi D, Blom J, Ali S, Ferry JG, Stingl U. Draft genome sequence of an obligately methylotrophic methanogen, *Methanococcoides methylutens*, isolated from marine sediment. Genome Announc. 2014;2:e01184–14.
78. Kellermann MY, Wegener G, Elvert M, Yoshinaga MY, Lin YS, Holler T, et al. Autotrophy as a predominant mode of carbon fixation in anaerobic methane-oxidizing microbial communities. Proc Natl Acad Sci USA. 2012;109:19321–6.
79. Weiss MC, Sousa FL, Mrnjavac N, Neukirchen S, Roettger M, Nelson-Sathi S, et al. The physiology and habitat of the last universal common ancestor. Nat Microbiol. 2016;1:16116.
80. Qin S, Sun Y, Tang Y. Early hydrocarbon generation of algae and influences of inorganic environments during low temperature simulation. Energy Explor Exploit. 2008;26:377–96.
81. Koga Y, Morii H. Biosynthesis of ether-type polar lipids in archaea and evolutionary considerations. Microbiol Mol Biol Rev. 2007;71:97–120.
82. Ekiel I, Sportt GD, Patel GB. Acetate and CO_2 assimilation by *Methanothrix concilii*. J Bacteriol. 1985;162:905–8.